10-29-2013

Peptide-Amphiphile Containing Arginine and Fatty Acyl Chains as Molecular Transporters

Amir Nasrolahi Shirazi
University of Rhode Island

Donghoon Oh
University of Rhode Island

Rakesh Kumar Tiwari
University of Rhode Island

Brian Sullivan
University of Rhode Island

Anju Gupta

See next page for additional authors

Peptide-Amphiphile Containing Arginine and Fatty Acyl Chains as Molecular Transporters

Authors

Amir Nasrolahi Shirazi, Donghoon Oh, Rakesh Kumar Tiwari, Brian Sullivan, Anju Gupta, Geoffrey D. Bothun, and Keykavous Parang

Peptide-Amphiphile Containing Arginine and Fatty Acyl Chains as Molecular Transporters

Amir Nasrolahi Shirazi,[1,2] Donghoon Oh,[1] Rakesh Kumar Tiwari,[1,2] Brian Sullivan,[1] Anju Gupta,[3] Geoffrey D. Bothun,[4] and Keykavous Parang[1,2,*]

[1]Department of Biomedical and Pharmaceutical Sciences, College of Pharmacy, University of Rhode Island, Kingston, Rhode Island 02881, United States

[2]School of Pharmacy, Chapman University, Orange, California 92866, United States

[3]Department of Biology and Chemistry, Department of Engineering, College of Arts and Sciences, Texas A&M International University, Laredo, Texas 78041, United States

[4]Department of Chemical Engineering, College of Engineering, University of Rhode Island, Kingston, Rhode Island 02881, United States

kparang@uri.edu

TITLE RUNNING HEAD. Peptide-Amphiphile as Drug Delivery Systems

*Corresponding author:

K. Parang: 7 Greenhouse Road, Department of Biomedical and Pharmaceutical Sciences, College of Pharmacy, University of Rhode Island, Kingston, Rhode Island, 02881, United States; Tel.: +1-401-874-4471; Fax: +1-401-874-5787; E-mail address: kparang@uri.edu

Table of Contents Graphic

PA1, n = 1
PA2, n =2

PA3, n = 1
PA4, n =2
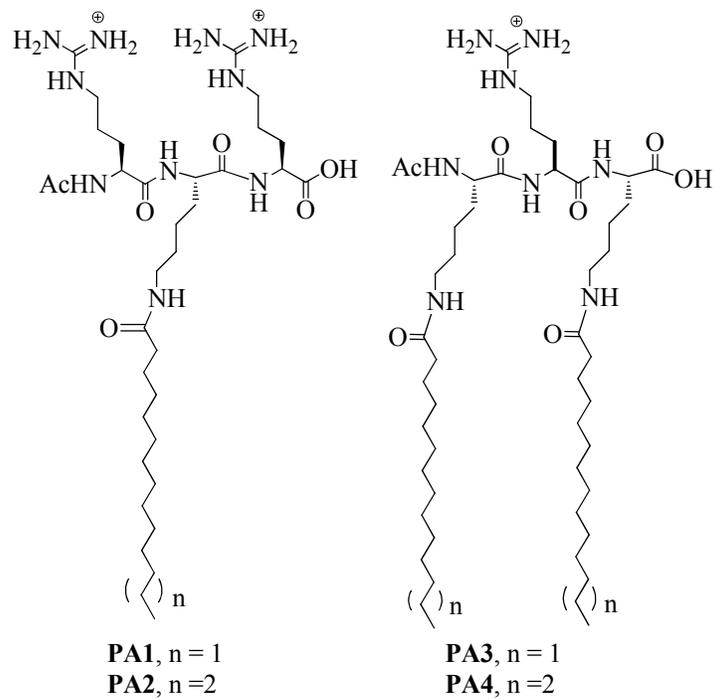
ABSTRACT

Peptide amphiphiles (PAs) are promising tools for the intracellular delivery of numerous drugs. PAs are known to be biodegradable systems. Here, four PA derivatives containing arginine and lysine conjugated with fatty acyl groups with different chain length, namely PA1: R-K(C_{14})-R, PA2: R-K(C_{16})-R, PA3: K(C_{14})-R-K(C_{14}), and PA4: K(C_{16})-R-K(C_{16}), where C_{16} = palmitic acid and C_{14} = myristic acid, were synthesized through Fmoc chemistry. Flow cytometry studies showed that among all synthesized PAs, only K(C_{16})-R-K(C_{16}), PA4 was able to enhance the cellular uptake of a fluorescence-labeled anti-HIV drug 2',3'-dideoxy-3'-thiacythidine (F′-3TC, F′ = fluorescein) and a biologically important phosphopeptide (F′-PEpYLGLD) in human leukemia cells (CCRF-CEM) after 2 h incubation. For example, the cellular uptake of F′-3TC and F′-PEpYLGLD was enhanced approximately 7.1- and 12.6-fold in the presence of the PA4 compared to those of the drugs alone. Confocal microscopy of F′-3TC and F′-PEpYLGLD loaded PA4 in live cells showed significantly higher intracellular localization than the drug alone in human ovarian cells (SK-OV-3) after 2 h incubation. The HPLC results showed that loading of Dox by the peptide amphiphile was 56% after 24 h. The loaded Dox was released (34%) within 48 h intracellularly. The CD results exhibited that the secondary structure of the peptide was changed upon interactions with Dox. Mechanistic studies revealed that endocytosis is the major pathway of the internalization. These studies suggest that PAs containing appropriate sequence of amino acids, chain length, charge, and hydrophobicity can be used as cellular delivery tools for transporting drugs and biomolecules.

Keywords: cellular uptake, drug delivery, nuclear targeting, peptide amphiphiles

INTRODUCTION

Drug Delivery Systems (DDS) have been employed to enhance the intracellular delivery of cargo molecules including drugs and biologically important molecules across the cellular membrane. Several factors can limit the cellular uptake of drugs, including degree of hydrophobicity, electrostatic charges, and molecular weight.[1]

Among all DDS, peptide amphiphiles (PAs) have been emerged as effective tools for drug transporting applications.[2] PAs are typically composed of hydrophobic and charged segments.[3] The lipophilic compartment can be synthesized by using either long chain fatty acids or amino acids carrying hydrophobic residues such as tryptophan (W), phenylalanine (F), and isoleucine (I) in the structure. The hydrophobic portion of PAs is responsible for the entrapment of drugs and enhances the permeability of the carrier into the cell membrane. Additionally, the positively charged block of the PAs is composed of cationic amino acids such as arginine (R) and lysine (K). The positively charged unit of PAs deals with its binding to negatively charged elements in the phospholipid membrane including heparin and phosphate moieties.[4,5]

Due to the biodegradability and bioactivity of PAs, they have been used for the delivery of a broad range of cargos including stem cells,[6] proteins,[7] oligonucleotides,[8] phosphopeptides,[9] and anticancer drugs.[10-13] Thus, the design and synthesis of novel PAs as highly efficient tools in modern drug delivery development have become a subject of major interest for researchers. PAs have been shown to improve the cellular uptake of various drugs through non-covalent entrapment. Because of unique properties of PAs, the loading and release of cargo molecules (drugs and/or biomolecules) are rapid since there is no covalent conjugation between the cargo molecules and the carrier. A simple physical mixing is sufficient for the loading of the cargo

molecules because the hydrophobic segments of PAs entrap the hydrophobic drug through non-covalent interaction. Another significant advantage of non-covalent loading approach is the smoothness of the release process. Due to the absence of the covalent binding between drug and carrier, the system does not suffer from issues related to unpredictable intracellular release of the conjugated drugs.[14] However, design and architecture of the charged amino acids sequence along with the degree of hydrophobicity are critical to control the function of the carrier. Several new therapeutic candidates are hydrophobic or anionic showing poor solubility in the aqueous phase or limited membrane translocation, respectivley.[15] Thus, design of novel PAs with optimal molecular transporter properties is urgently needed.

We have previously reported the design and synthesis of short cationic linear peptide analogs (LPAs, prepared as Arg-C_n-Arg-C_n-Lys, where C_n represented an alkyl chain containing $n = 5$, 7, or 11 methylenes). Among all synthesized peptides, a fluorescently conjugated LPA-C_{11} (F′-LPA-C_{11}) demonstrated significant cellular uptake compared to the shorter LPAs. Thus, we have found that the chemical, physical, and biological properties of LPAs can be controlled by manipulating the chain length in the backbone and number or sequence of amino acids in the structure.[14] However, no study was performed on the role of the side chain manipulation of the amino acids.

To address the question that whether the side chain length can affect the cellular penetration of the PAs, four PAs derivatives containing arginine and lysine conjugated with fatty acyl groups of different chain lengths namely PA1: R-K(C_{14})-R, PA2: R-K(C_{16})-R, PA3: K(C_{14})-R-K(C_{14}), and PA4: K(C_{16})-R-K(C_{16}), where C_{16} = palmitic acid and C_{14} = myristic acid, were synthesized through Fmoc chemistry. The presence of two C_{16} chains was found to be critical for

the PAs transporter activity. To the best of our knowledge, this is the first report of the synthesis and comparative biological evaluation of PAs of this class.

EXPERIMENTAL SECTION

General

Reactions were carried out in Bio-Rad polypropylene columns by shaking and mixing using a Glass-Col small tube rotator under dry conditions at room temperature. PAs were synthesized by solid-phase synthesis using *N*-(9-fluorenyl)methoxycarbonyl(Fmoc)-based chemistry and employing Fmoc-L-amino acid building blocks. Fmoc-Lys(Mtt)-Wang resin (1 g, 0.35 mmol/g) and Fmoc-Arg(Pbf)-Wang resin (1 g, 0.35 mmol/g) were used as starting amino acids. For the coupling of next amino acids, Fmoc-Arg(Pbf)-OH and Fmoc-Lys(Mtt)-OH were used alternatively. 2-(1*H*-Benzotriazole-1-yl)-1,1,3,3-tetramethyluronium hexafluorophosphate (HBTU) and *N,N*-diisopropylethylamine (DIPEA) in *N,N*-dimethylformamide (DMF) were used as coupling and activating reagents, respectively. Wang resin loaded Fmoc amino acid, coupling reagents, and Fmoc-amino acid building blocks were purchased from Chempep (Miami, FL). Other chemicals and reagents were purchased from Sigma-Aldrich Chemical Co. (Milwaukee, WI). Fmoc deprotection at each step was carried out using piperidine in DMF (20%). The crude peptides were purified by using a reversed-phase Hitachi HPLC (L-2455) on a ZORBAX SB-C3 column, (4.6 mm × 25 cm, 5 µm) and a gradient system. The peptides were separated by eluting the crude peptides at 10.0 mL/min using a gradient of 0-100% acetonitrile (0.1% trifluoroacetic acid (TFA)) and water (0.1% TFA) over 60 min, and then were lyophilized to yield cyclic peptides. The purity of final products (≥95%) was confirmed by analytical HPLC. The analytical HPLC was performed on a Hitachi analytical HPLC system using a C18 Shimadzu Premier 3 µm

column (150 cm × 4.6 mm) and a gradient system (H_2O/CH_3CN), and a flow rate of 1 mL/min with detection at 220 nm. The chemical structures of final products were confirmed by high-resolution MALDI AXIMA performance TOF/TOF mass spectrometer (Shimadzu Biotech) or a high-resolution Biosystems QStar Elite time-of-flight electrospray mass spectrometer. As a representative example, the synthesis of K(C$_{16}$)-R-K(C$_{16}$) is outlined here.

Synthesis of K(C$_{16}$)-R-K(C$_{16}$) Peptide Amphiphile (PA4).

Fmoc-Lys(Mtt)-Wang resin (1 g, 0.35 mmol/g) was swelled in anhydrous DMF for approximately 30 min under dry nitrogen. The excess of the solvent was filtered off. The swelling and filtration steps were repeated for 2 more times before the coupling reactions. Fmoc-Arg(Pbf)-OH (325 mg, 0.75 mmol) and Fmoc-Lys(Mtt)-OH (325 mg, 0.75 mmol) were coupled to the *N*-terminal of lysine Wang resin in the presence of HBTU (285 mg, 0.75 mmol) and DIPEA (262 μL, 1.50 mmol) in DMF (7 mL) by mixing for 1.5 h. After the coupling was completed, the reaction solution was filtered off, and the resin was collected by filtration and washed with DMF (7 × 15 mL), followed by *N*-terminal Fmoc deprotection using piperidine in DMF (20% v/v, 10 mL, 2 times, 5 and 10 min). The *N*-terminal of the linear peptide was coupled with acetic anhydride (0.5 mL, 5 mmol) using DIPEA (285 mg, 0.75 mmol). The lysine protecting groups (*N*-methyltrityl, Mtt) were removed by using trifluoroacetic acid (TFA, 5%) in dichloromethane (DCM, 15 mL). This cleavage reaction was carried out for 10 min and repeated for three times (3 × 10 min) to confirm that all the Mtt groups were removed. After the deprotection of Mtt groups, the coupling of myristoyl or palmitoyl chloride (1 mmol, 305 μL) with the free side chains of lysine was carried out using DIPEA in DCM as a coupling reagent for 3 h. The 2,2,4,6,7-pentamethyldihydrobenzofuran-5-sulfonyl (Pbf) side chain deprotection

7

was accomplished with the mixture of TFA (13.5 mL)/thioanisole (750 µL)/anisole (300 µL)/DTT (450 mg) for 2 h. The peptide was separated by eluting the crude peptides at 10.0 mL/min using a gradient of 0-100% acetonitrile (0.1% TFA) and water (0.1% TFA) over 60 min, and then was lyophilized.

R-K(C$_{14}$)-R-Ac, PA1: HR-MS (ESI-TOF) (m/z): C$_{34}$H$_{66}$N$_{10}$O$_6$ calcd, 710.5295; found, 711.4881 [M + H]$^+$. **R-K(C$_{16}$)-R-Ac, PA2:** HR-MS (ESI-TOF) (m/z): C$_{36}$H$_{70}$N$_{10}$O$_6$ calcd, 738.5539; found, 739.1488 [M + H]$^+$. **K(C$_{14}$)-R-K(C$_{14}$)-Ac, PA3:** HR-MS (ESI-TOF) (m/z): C$_{48}$H$_{92}$N$_8$O$_7$ calcd, 893.7162; found, 898.7239 [M + H]$^+$. **K(C$_{16}$)-R-K(C$_{16}$)-Ac, PA4:** HR-MS (ESI-TOF) (m/z): C$_{52}$H$_{101}$N$_8$O$_7$ calcd, 948.7715; found, 949.7364 [M + H]$^+$.

Fluorescently-Labeled Conjugate of PA4 (F′-K(C$_{16}$)-R-K(C$_{16}$) [F′-PA4]). F′-K(C$_{16}$)-R-K(C$_{16}$) [F′-PA4] was synthesized using Fmoc-Lys(Mtt)-Wang resin (loading 0.35 mmol/g, 0.5 mmole, 1.43 g). The Fmoc group was deprotected using 20% piperidine followed by coupling with Fmoc-Arg(Pbf)-OH. The amino acid sequence was assembled followed by the deprotection of the attached Fmoc group to the *N*-terminal. The free NH$_2$ group was coupled with Fmoc-βAla-OH on the resin to be used as a linker. After the lysine side chain orthogonal protection, the Mtt groups were deprotected on the solid phase resin using a cleavage cocktail, TFA: triisoproylsilane (TIS):DCM (5:10:85, *v/v/v*, 20 mL, 3 times × 10 min each) followed by washing the resin with DCM (3 times, 25 mL) and DMF (3 × 25 mL). The free amino group was conjugated with palmitoyl chloride (8 equiv, 1222 µL) in the presence of DIPEA (16 equiv, 1393 uL) by using DMF (20 mL). The resin was washed with DMF (3 × 25 mL) and DCM (3 × 25 mL), and finally the Fmoc group of the *N*-terminal was deprotected and further conjugated with

the peptidyl resin containing 5(6)-carboxyfluorescein isobutyrate (CFDI) (2.5 equiv, 652 mg), in the presence of HOAt (2.5 equiv, 168 mg), 7-azabenzotriazol-1-yloxy) tripyrrolidinophosphonium hexafluorophosphate (PyAOP, 2.5 equiv, 648 mg), and *N,N*-diisopropylethylamine (DIPEA) (5 equiv, 522 µL) in DMF:DCM (4:2 v/v, 12 mL) for 2 h followed by washing and cleavage of isobutyrate protection in CFDI by agitating the peptidyl resin using piperidine (25 mL, 2 × 20 min). The resin was finally washed with DMF (3 × 25 mL), DCM (3 × 25 mL), MeOH (25 mL× 3) and finally dried in vacuum for overnight before final cleavage. The deprotection of the Pbf group of arginine side chain and cleavage of final peptide from the solid phase was performed in the presence of freshly prepared reagent R (TFA/thioanisole/anisole/ethanedithiol, 90:5:3:2 v/v/v/v, 12 mL) after 1.5 h shaking followed by the evaporation of the cleavage cocktail in rotary evaporator to afford the crude oily liquid. The crude product that was purified by reversed-phase HPLC by using ZORBAX SB-C3 column, (4.6 mm × 25 cm, 5 µm) to afford the final product. The structures of the final compound were confirmed by high-resolution MALDI TOF/TOF mass spectrometry. MALDI-TOF (*m/z*) [$C_{74}H_{117}N_9O_{13}$]: calcd, 1339.8771; found, 1337.8620 [M-2H][2].

Cell Culture. Human leukemia cell line CCRF-CEM (ATCC no. CCL-119), ovarian carcinoma SK-OV-3 (ATCC no HTB-77), and colon carcinoma HCT-116 (ATCC no. CCL-247) were obtained from American Type Culture Collection. Cells were grown on 75 cm^2 cell culture flasks with RPMI-16 medium (for leukemia cells) and EMEM medium (for SK-OV-3 and HCT-116 cells), supplemented with 10% fetal bovine serum (FBS), and 1% penicillin-streptomycin solution (10,000 units of penicillin and 10 mg of streptomycin in 0.9 % NaCl) in a humidified atmosphere of 5% CO_2, 95% air at 37 ºC.

Cytotoxicity Assay. SK-OV-3 (5,000), HCT-116 (4,000) and CCRF-CEM (30,000) cells were seeded in 0.1 mL per well in 96-well plates 24 h prior to the experiment. The old medium (EMEM containing FBS (10%)) was replaced (not in case of CCRF-CEM) by different concentrations (10-100 µM) of PA1, PA2, PA3 or PA4 in serum containing medium and incubated for 24 h at 37 °C in a humidified atmosphere of 5% CO_2. Cell viability was then determined by measuring the fluorescence intensity at 490 nm using a SpectraMax M2 microplate spectrophotometer. The percentage of cell survival was calculated as [(OD value of cells treated with the test mixture of compounds) − (OD value of culture medium)]/[(OD value of control cells) − (OD value of culture medium)] × 100%.

Flow Cytometry Studies. CCRF-CEM (1×10^7 cells) was taken in 6-well plates in serum-free RPMI medium. Then the fluorescence-labeled compound including F′-3TC or F′-PE(pY)LGLD) (5 µM) was added to the different wells containing PA1 (50 µM), PA2 (50 µM), PA3 (50 µM), and PA4 (50 µM) in serum-free media. The plates were incubated for 2 h at 37 °C. Cells and fluorescence-labeled compounds alone were used as negative controls. After 2 h incubation, the media containing the peptide was removed. The cells were digested with 0.25% trypsin/EDTA (0.53 mM) for 5 min to remove any artificial surface binding. Then the cells were washed twice with PBS. Finally, the cells were resuspended in flow cytometry buffer and analyzed by flow cytometry (FACSCalibur™: Becton Dickinson) using FITC channel and CellQuest software. The data presented were based on the mean fluorescence signal for 10,000 cells collected. All assays were performed in triplicate.

To perform the time-dependent assay, CCRF-CEM (1×10^7 cells) was taken in 6-well plates in serum-free RPMI medium. Then the fluorescence-labeled PA, F′-PA4 (5 µM), was added to the different wells in serum-free media at different periods of time. The plates were incubated for 10 min, 30 min, 1 h, and 2 h at 37 °C. Cells and 5-(6)-carboxyfluorescein (FAM, 5 µM) were used as negative controls. After the desired incubation time, the media containing the fluorescently-labeled peptide was removed. The washing procedure and instrument settings of the experiment were carried out as described above.

Cellular Uptake Studies in the Presence of Inhibitors. Human leukemia adenocarcinoma cells (CCRF-CEM) were seeded in six well plates (1×10^7 cells/well) in serum-free RPMI medium. The cells were pre-incubated by various inhibitors including, nystatin (50 µg/ml), chloroquine (100 µM), chlorpromazine (30 µM), methyl-β-cyclodextrin (2.5 mM), and 5-(N-ethyl-N-isopropyl)amiloride (EIA, 50 µM) for 30 min. Then, the fluorescence labeled PA4 (F′-PA4, 5 µM) was added into cells. The treatment was continued for 2 h at 37 ºC. Consequently, similar FACS protocol was performed as described above.

Confocal Microscopy on Live Cells. Adherent SK-OV-3 cells were seeded with EMEM media overnight on coverslips in six well plates (1×10^5 cells per well). Then, the media were removed and washed with opti-MEM. The cells were treated with the mixture of fluorescence-labeled compounds including either F′-3TC or F′-PE(pY)LGLD (5 µM) in the presence and absence of PA4 (50 µM) in opti-MEM for 2 h at 37 ºC. For microscope studies of F′-PA4, only fluorescence labeled peptide (5 µM) was incubated with cells and FAM (5 µM) was used as a negative control. After 2 h incubation, the media containing the treatments were removed followed by

washing with PBS three times. The coverslips were mounted on a microscope slide with mounting media with cells-attached side facing down. Laser scanning confocal microscopy was carried out using Carl Zeiss LSM 700 system. The cells were imaged using fluorescein isothiocyanate (FITC), diamidino-2-phenylindole (DAPI) and differential interference contrast (DIC) channels. The fluorescence images were taken under 20 × objective. Blue and green luminescent emissions from DAPI and FITC were excited at the wavelength of 405 nm and 488 nm, respectively. The emission wavelengths were ranged from 425 nm to 475 nm for DAPI and 500 nm to 550 nm for FITC. There was no interference between these two channels. The scanning mode was in sequential frame.

Circular Dichroism. CD spectra were recorded on a JASCO J-810 spectropolarimeter using 1 mm path length cuvettes. The scan speed was 100 nm/min, and spectra were averaged over 8 scans. All experiments on the samples including PA4 (50 µM, H_2O) and PEpYLGLD or Dox (10 µM, H_2O) were tested at room temperature. The CD for background reference (water) was measured and subtracted from the sample.

Drug Loading. Doxorubicin (Dox) aqueous solution (100 µL, 200 µM) was added into PA4 solution (400 µL, 500 µM) with the concentration ratio of Dox to PA 1:10. The mixture was transferred into a 1 mL dialysis membrane (with the cutoff molecular weight 1000 D; Float-A-Lyzer G2, Spectrum Labs). The membrane was sealed and submerged into water (500 mL) as a medium. After stirring in dark for 24 h, unloaded Dox in the mixture was collected and evaporated to reduce the volume. The concentration of Dox was measured using a reverse phase HPLC system installed with Hitachi premier C18 3 µm, 4.6 × 150 mm column at UV/Vis 490

12

nm wavelength. Mobile phases were water with 0.1% trifluoroacetic acid and acetronitrile with 0.1% trifluoroacetic acid. The gradient from 10 to 90% acetonitrile was applied to separate the Dox peak from other impurities. The calibration standard solutions were injected to quantify Dox in the sample solution. The loading efficiency was calculated using the following equation:

$$\text{Loading efficiency (wt/wt, \%)} = \frac{\text{Dox in feed} - \text{free Dox}}{\text{Dox in feed}} \times 100$$

Cellular Release. Intracellular release and accumulation of Dox were determined in CCRF-CEM cells by HPLC analysis. CCRF-CEM cells were grown in 75 cm^2 culture flasks with RPMI medium (containing 10% FBS and 1% penicillin-streptomycin) to achieve ~70−80% confluence (1×10^7 cells/mL). The cells were partitioned/transferred to culture plates (six well) having 1×10^7 cells per well in 2 mL of medium. The treatment in fresh RPMI medium containing Dox-PA4 (5:50 μM) was added to cells, and the incubation was continued at 37 °C for different times (2, 12, 24, and 48 h). After the incubation time, the cells were collected by centrifugation. The medium was removed, and cell pellets were washed with ice-cold PBS (5 mL) twice to remove any medium. The cell pellets were thoroughly extracted with an equal volume of methanol, chloroform, and isopropanol mixture (4:3:1 v/v/v) and filtered through 0.2 μm filters. The solvents were evaporated under N$_2$ gas. The released Dox was quantified by reverse phase HPLC system with UV/Vis detector (490 nm). The HPLC condition was similar to what was described before in drug loading section.

Antiproliferative Assay. The antiproliferative activity of Dox alone and in the presence of PA-4 against SK-OV-3 cells was determined by MTS assay. All cells were plated overnight in 96-well plates with a density of 5000 cells per well in 0.1 mL of appropriate growth medium at 37 °C. Dox alone (5 μM) or a combination of Dox (5 μM) and PA4 (25 μM) were incubated with the cells for 4 h. Excess of compounds was removed and washed by fresh media. The cells were kept in an incubator for 24 h. The cells without compounds were included in each experiment as controls. After 24 h incubation, 20 μL of MTS solution was added and incubated for 2 h. The absorbance of the formazan product was measured at 490 nm using a microplate reader. The percentage of cell viability was calculated as (OD value of untreated cells − OD value of treated cells)/OD value of untreated cells × 100%.

RESULTS AND DISCUSSION

Chemistry

Four PAs containing arginine and lysine conjugated with lipophilic carbon chains including PA1: Ac-Arg-Lys(C_{14})-Arg-OH = Ac-R-K(C_{14})-R, PA2: Ac-Arg-Lys(C_{16})-Arg = R-K(C_{16})-R, PA3: Ac-Lys(C_{14})-Arg-Lys(C_{14})-OH = Ac-K(C_{14})-R-K(C_{14})-OH, and PA4: Ac-Lys(C_{16})-Arg-Lys(C_{16})-OH = Ac-K(C_{16})-R-K(C_{16})-OH (Figure 1) were synthesized by using 9-fluorenylmethyoxycarbonyl (Fmoc)-based chemistry.[16,17]
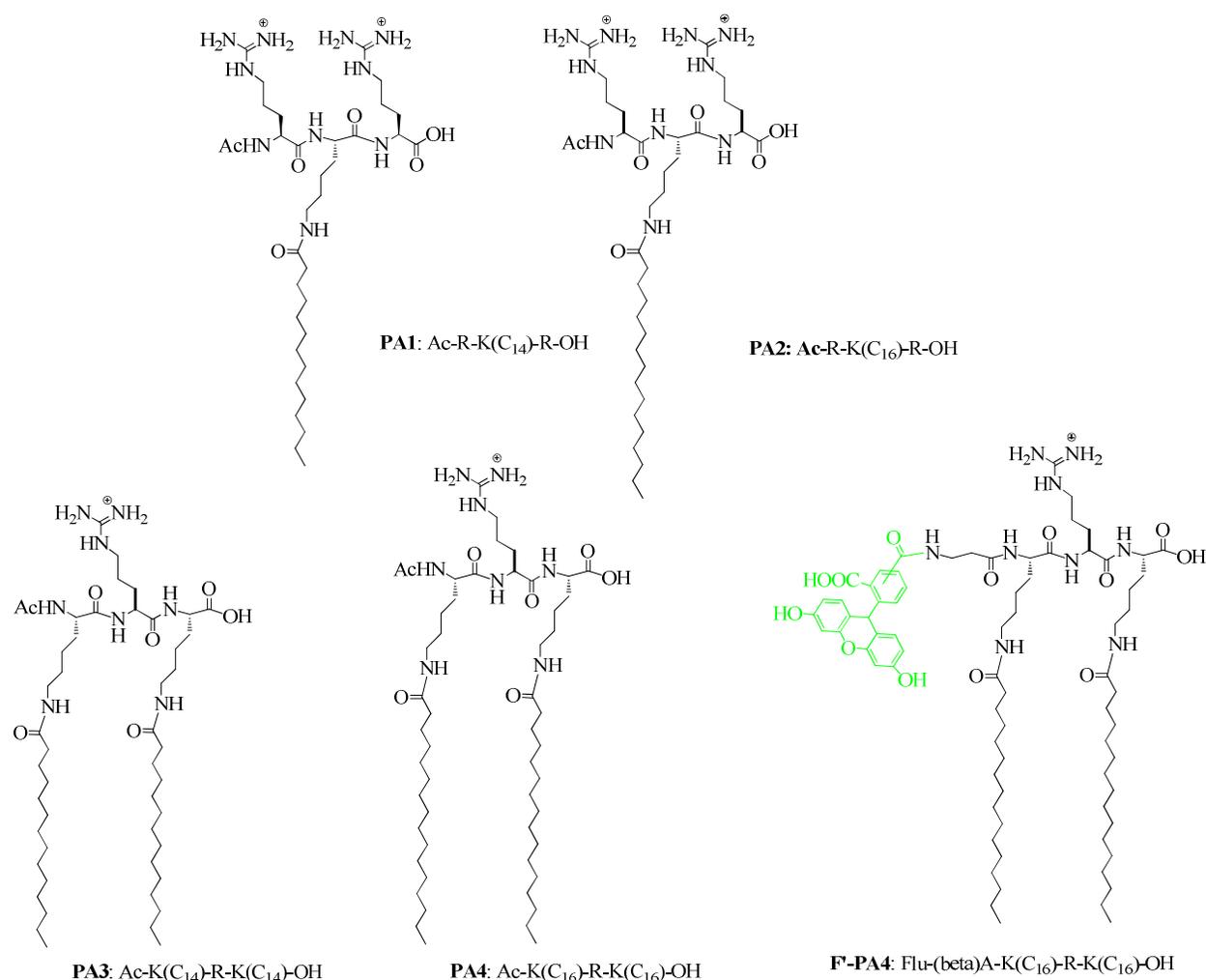
Figure 1. Chemical structures of synthesized PAs and fluorescence=labeled PA4.

As representative examples, the synthesis of PA3 and PA4 was performed by assembling the peptide on the NH_2-K(Mtt)-Wang resin followed by *N*-terminal Fmoc deprotection using piperidine in DMF (20 %, v/v). Subsequently, the free *N*-terminal was capped by acetic anhydride (0.5 mL, 5 equiv). At the next step, all Mtt protecting groups of lysine were removed by using trifluoroacetic acid in DCM (10 %, v/v). After washing the free lysine with DCM, the conjugation with either myristoyl chloride or palmitoyl chloride was performed in the presence

of DIPEA. The cleavage of the peptide from the resin was carried out using the cleavage cocktail

containing (TFA/thioanisole/anisole/DTT, 90:5:3:2 v/v/v/v). The crude product was purified by

HPLC to afford the pure PA3 or PA4 (Scheme 1). All other PAs were synthesized using a similar

protocol using appropriate resins.
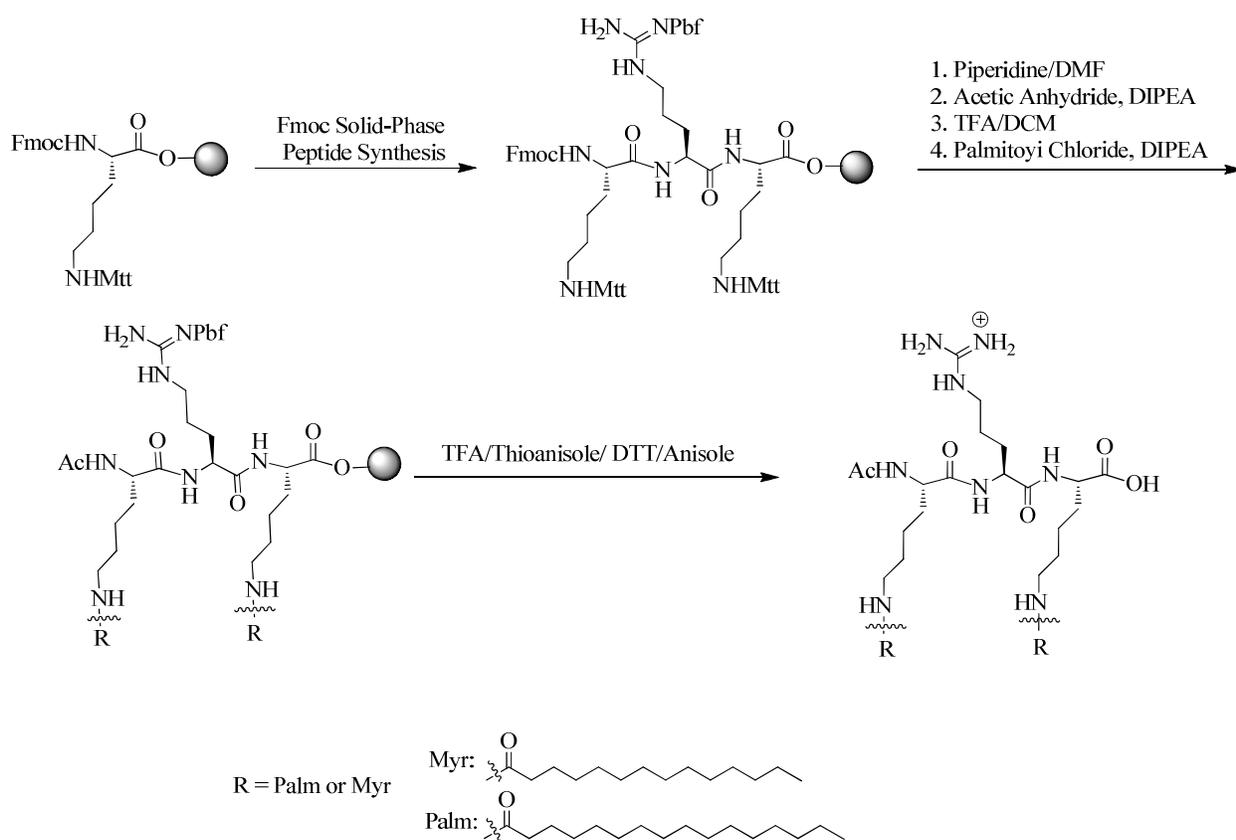
Scheme 1. Solid-phase synthesis of PA3 and PA4.

The fluorescent-labeled compounds were synthesized according to the procedure that

described above with some partial modification (Scheme 2). F′-K(C$_{16}$)-R-K(C$_{16}$) [F′-PA4] was

synthesized using Fmoc-Lys(Mtt)-Wang resin (loading 0.35 mmol/g). The Fmoc group was

deprotected using 20% piperidine followed by coupling with Fmoc-Arg(Pbf)-OH. The amino acid sequence was assembled followed by the deprotection of the attached Fmoc group to the *N*-terminal. The free NH_2 group was coupled with Fmoc-βAla-OH on the resin to be used as a linker. The Mtt groups of lysine were deprotected on the solid phase resin using a cleavage cocktail (TFA:TIS:DCM (5:10:85, *v/v/v*, 20 mL). The free amino group was conjugated with palmitoyl chloride in the presence of DIPEA by using DMF (20 mL). Finally the Fmoc group of the *N*-terminal was deprotected and further conjugated with the peptidyl resin containing (CFDI (2.5 equiv), in the presence of HOAt (2.5 equiv), PyAOP (2.5 equiv), and DIPEA (5 equiv) in DMF:DCM (4:2 v/v) for 2 h followed by washing and cleavage of isobutyrate protection in CFDI by agitating the peptidyl resin using piperidine (25 mL). The deprotection of the Pbf group of arginine side chain and cleavage of final peptide from the solid phase was performed in the presence of freshly prepared reagent R (TFA/thioanisole/anisole/ethanedithiol, 90:5:3:2 v/v/v/v) after 1.5 h shaking followed by the evaporation of the cleavage cocktail to afford the crude oily liquid. The crude product that was purified by reversed-phase HPLC to afford the final product.
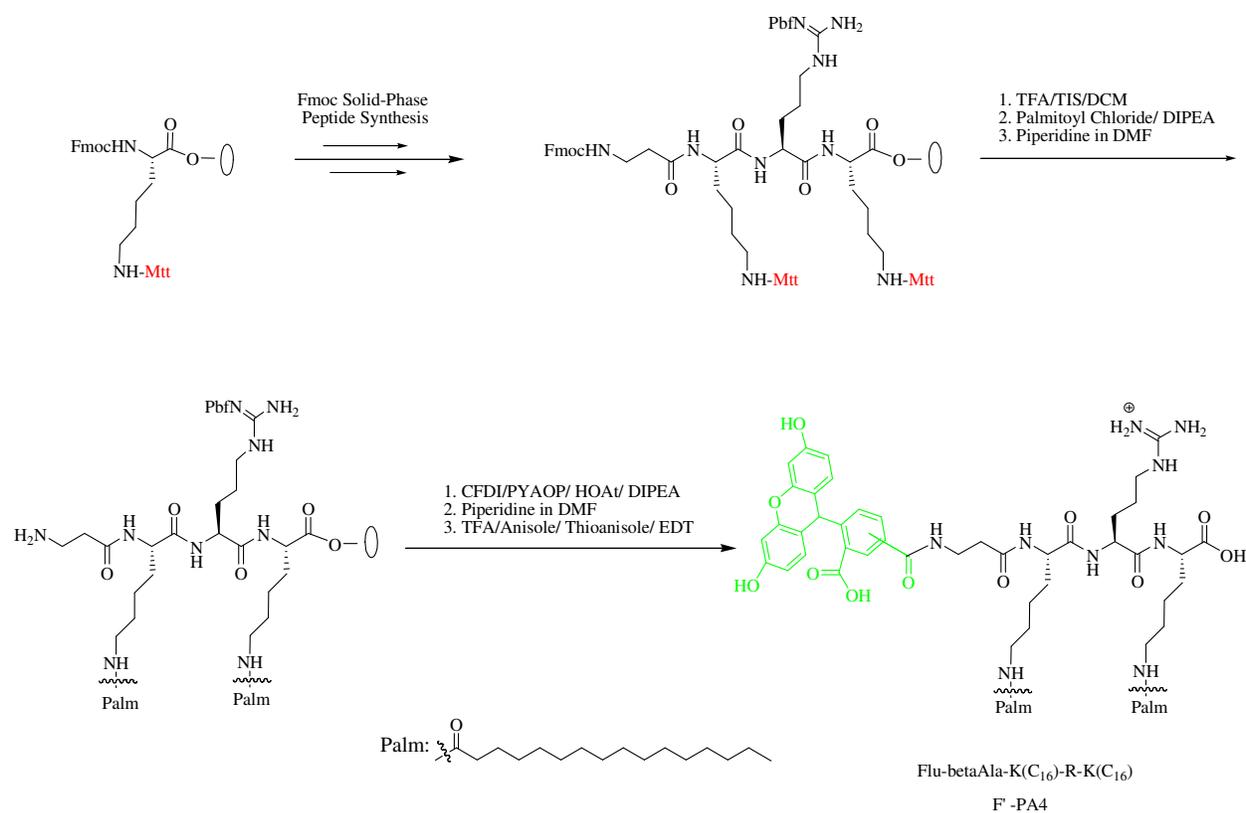
Scheme 2. Solid-phase synthesis of fluorescence-labeled PA4.

Cytotoxicity of PAs

The cytotoxicity of all synthesized PAs were evaluated in SK-OV-3, CCRF-CEM, and HCT-116 cancer cells at different concentrations (10-100 μM) after 24 h incubation time (**Figure S1**). Among all PAs, PA4 was found to be less toxic compared to other PAs reducing cell proliferation by 12, 3, and 1% in CCRF-CEM, HCT-116, and SK-OV-3 cell lines at a concentration of 100 μM, respectively. Among all PAs, PA1 showed higher toxicity reducing cell proliferation of HCT-116, CCRF-CEM, and SK-OV-3 cells by 15, 20, and 24% in respectively. Similarly, the cytotoxicity results at 50 μM of PAs showed that increasing the number of aliphatic side chains reduces the toxicity of the peptide and the compounds were less

toxic at this concentration (Figure 2). The concentration of 50 μM of PAs was used for further cell-based studies.
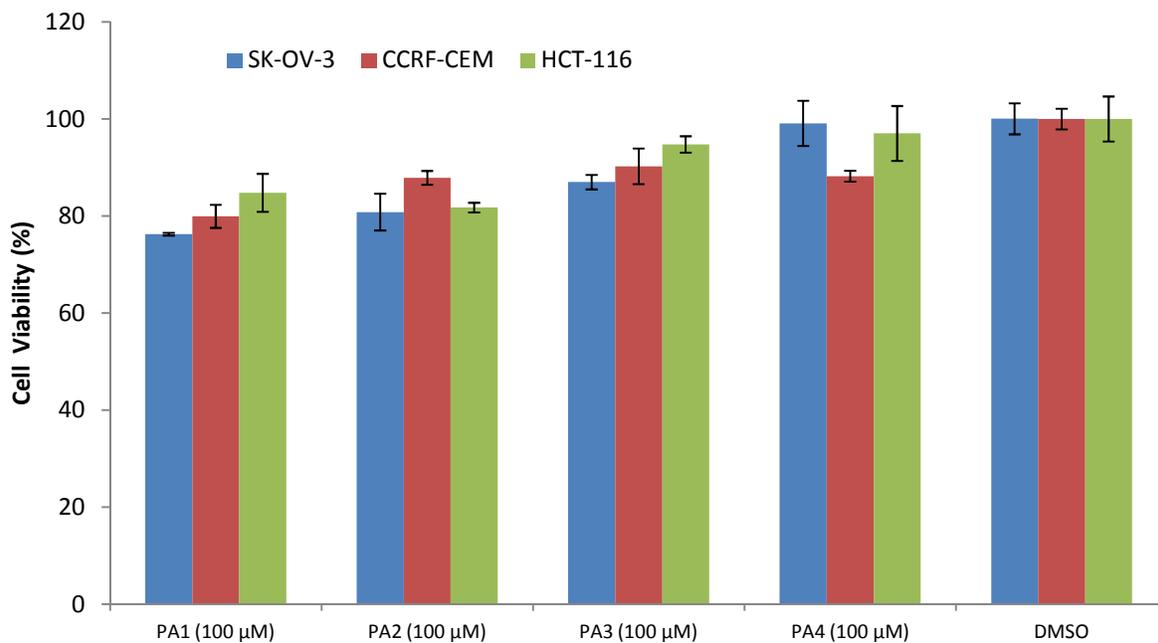

Figure 2. Cytotoxicity of PAs (100 μM) after 24 h incubation with SK-OV-3, HCT-116, and CCRF-CEM cells.

Drug Loading

Dox was used as a model drug for the quantitative loading studies. The loading of Dox was carried out based on previously reported method.[18] Dox solution (100 μL, 100 μM) was mixed with PA4 solution (400 μL, 500 μM) to obtain 1:10 molar ratio. A dialysis membrane was used to quantify the amount of the unloaded Dox. After 24 h stirring in water as media around the dialysis bag, the loading efficiency was found to be 56.7%. These data indicate that PA4 has

a potential to be further examined for molecular transporting property because of high entrapment of Dox after 24 h

Cellular Uptake Studies

Evaluation of PA4 as a Molecular Transporter

To evaluate PAs as molecular transporters, a model experiment with an anti-HIV drug, 3TC, as a cargo drug was performed. 3TC works as a nucleoside reverse transcriptase inhibitor blocking HIV-1 and hepatitis B virus (HBV) replication.[19] The efficient cellular uptake of 3TC is critical for anti-HIV activity. To monitor the molecular transporter ability of PAs, a carboxyfluorescein derivative of 3TC (F′-3TC) was synthesized as described previously.[20,21]

CCRF-CEM cells were incubated with F′-3TC (5 µM) in the presence or absence of PA1, PA2, PA3, and PA4 (50 µM) for 2 h at 37 ºC and then was treated with trypsin to remove cell surface-bound drugs. Intracellular uptake of F′-3TC (5 µM) was measured in cells using fluorescence activated cell sorter (FACS). FACS showed significantly higher fluorescence signals in cells treated with F′-drug-loaded PA4 compared to F′-drug-loaded PA1, PA2, PA3, and drug alone. The cellular uptake of F′-drug-loaded PA4 was found to be 7.1-fold higher than F′-3TC alone (Figure 3). However, the cellular uptake of F′-3TC in the presence of PA1, PA2, and PA3 only improved by 1.1-, 1.3- and 2.5-fold compared to that of the drug alone. PA4 enhanced the uptake of the drug dramatically, possibly because of the appropriate amino acids and lipophilic chain along with proper length (C_{16}) in the structure of PA4. These data suggest that PAs with the right balance between the charged and hydrophobic residues and sufficient hydrophobicity to for drug entrapment can work as a molecular transporter.
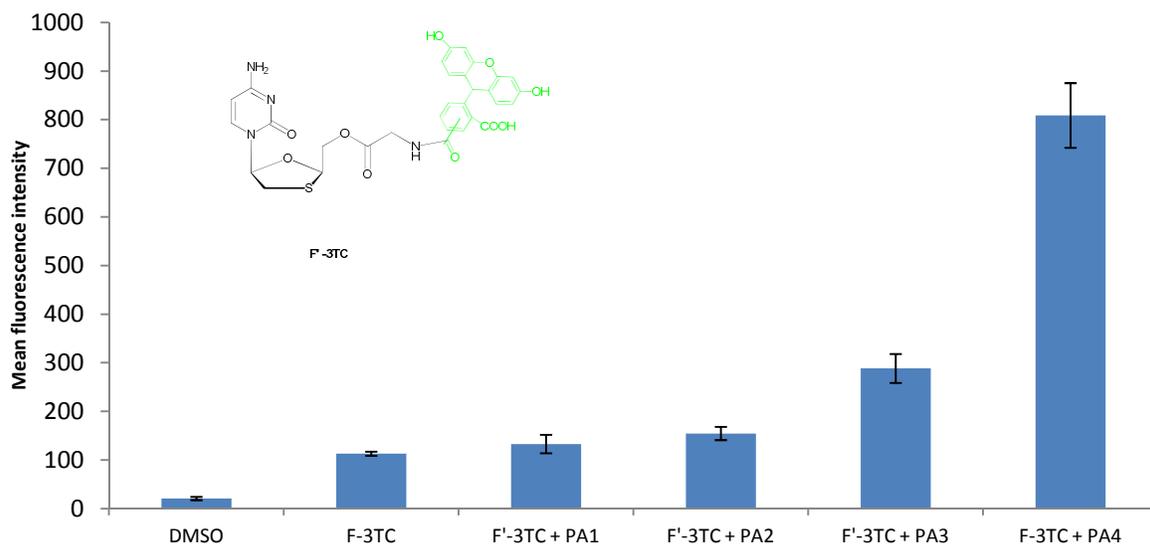
Figure 3. Cellular uptake studies for F′-3TC (5 µM) in the presence of PAs (50 µM) after 2 h incubation.

To visualize the enhancement of the cellular uptake of drugs, F′-3TC was used as a model for confocal microscopy in SK-OV-3 cells. Confocal microscopy showed that F′-3TC–loaded PA4 gets localized mostly in the cytoplasm of cells compared to drug alone. The incubation of cells with F′-3TC alone did not show any fluorescence intensity in cells. These data confirm that the presence of the peptide enhanced the cellular permeability (Figure 4) and the delivery of the nucleoside cargo.
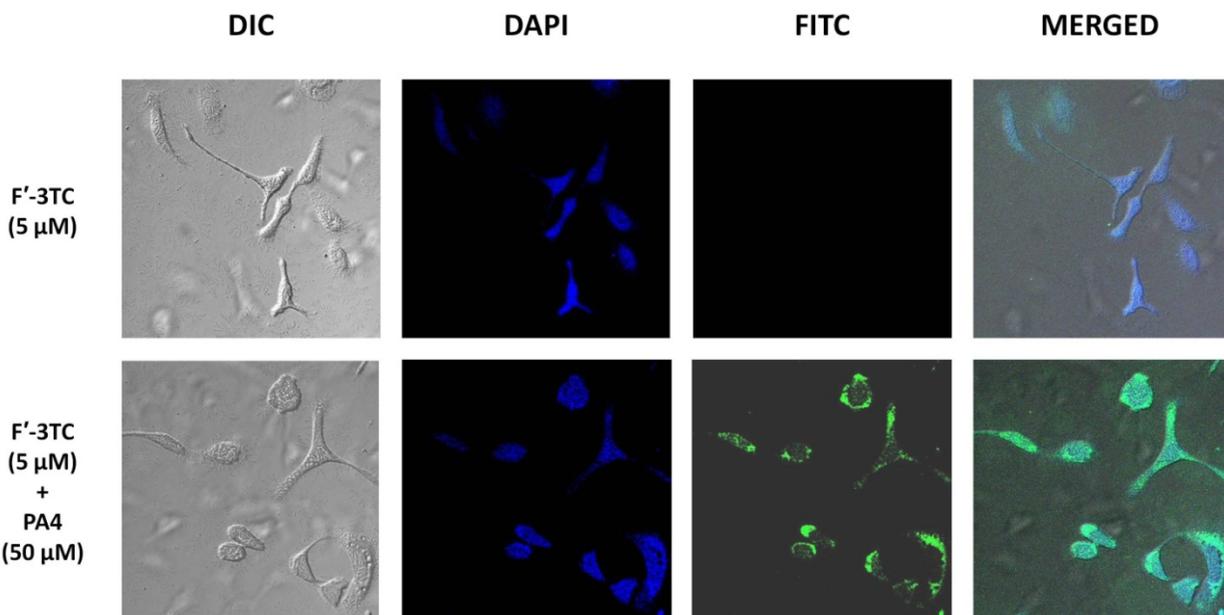
Figure 4. Confocal microscope images of F′-3TC (5 μM) uptake by SK-OV-3 cells in the presence of PA4 (50 μM) after 2 h incubation.

The molecular transporting efficiency of PA4 for the delivery of large-sized biomolecules was evaluated by using a cell-impermeable negatively charged phosphopeptide as a model biomolecule using flow cytometry. Although phosphopeptides are valuable probes for studying the protein-protein interactions, they have found limited applications due to their low cell permeability. They do not cross the cell-membrane readily because of the presence of the negatively charged phosphate group. PEpYLGLD is a sequence that mimics the pTyr[1246] of ErbB2 and is responsible binding to the Chk SH2 domain.[22] The cellular uptake of F′-PEpYLGLD was monitored in the presence of all PAs including PA1, PA2, PA3, and PA4 in CCRF-CEM cells. FACS analysis showed that among all PAs, PA4 enhanced the uptake of F′-PEpYLGLD by 12.6-fold compared to that of the drug alone, suggesting that this system could

function as a delivery tool for F′-PEpYLGLD (Figure 5). However, the cellular uptake of F′-PEpYLGLD was not enhanced in the presence of other PAs, such as PA1, PA2, or PA3. These results are consistent with the cellular uptake studies of lamivudine that described above, confirming the potential of PA4 in improving the cellular uptake
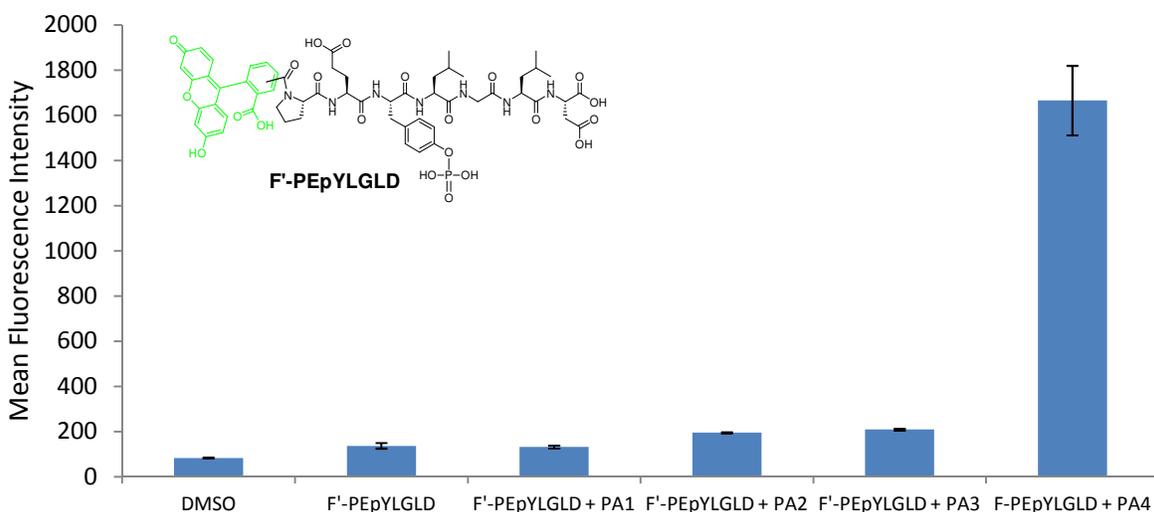

Figure 5. Cellular uptake of F′-PEpYLGLD (5 μM) in the presence of PAs after 2 h incubation.

Considering the significant enhancement of F′-PEpYLGLD in the presence of PA4 (Figure 5), confocal microscopy was used to confirm the cellular uptake of this negatively charged phosphopeptide in the presence and absence of this PA. Thus, confocal microscopy was conducted by measuring the fluorescence intensity of F′-PEpYLGLD-loaded PA4 compared to F′-PEpYLGLD alone in SK-OV-3 cells after 2 h incubation. DAPI was employed to stain the nucleus. The cells were incubated with F′-PEpYLGLD-loaded PA4 and F′-PEpYLGLD alone. No green fluorescence was observed for the parent fluorescence-labeled phosphopeptide, suggesting that F′-PEpYLGLD alone did not cross the membrane because of the presence of negatively charged phosphate group in the structure. As it is shown in Figure 6, the cell nuclei

stained by DAPI (blue) were circumvented by the green fluorescence showing the fluorescent-labeled phosphopeptide localized in the cytoplasm in the presence of PA4. These results indicated that the presence of PA4 is critical to improve the cellular uptake of the cell-impermeable phosphopeptide. However, there was no evidence that the PA can internalize into cells. To address this question, the fluorescence labeled PA4 was synthesized and was used for further cellular uptake investigations.
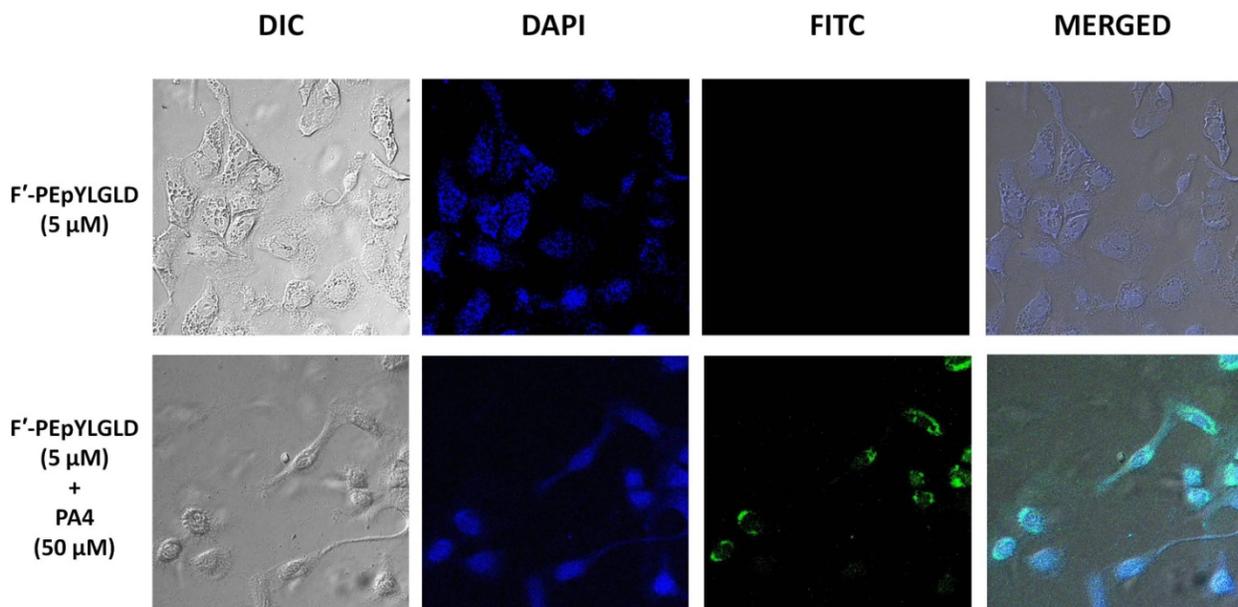

Figure 6. Confocal microscope images of F′-PEpYLGLD (5 μM) uptake by SK-OV-3 cells in the presence of PA4 (50 μM) after 2 h incubation.

Cellular Uptake of PA4

To confirm the internalization of PA4 alone, fluorescence-labeled PA4 (F′-PA4), F′-K(C$_{16}$)-R-K(C$_{16}$), was prepared as described above. Incubation of F′-PA4 (5 μM) with CCRF-CEM cells for 2 h showed 7.5-fold higher cellular uptake compared to the FAM (5 μM) alone,

thus suggesting the peptide structure is crucial for enhanced intracellular permeability (Figure 7). The cellular uptake of F′-PA4 was found to be time-dependent and rapid even after 10 min.
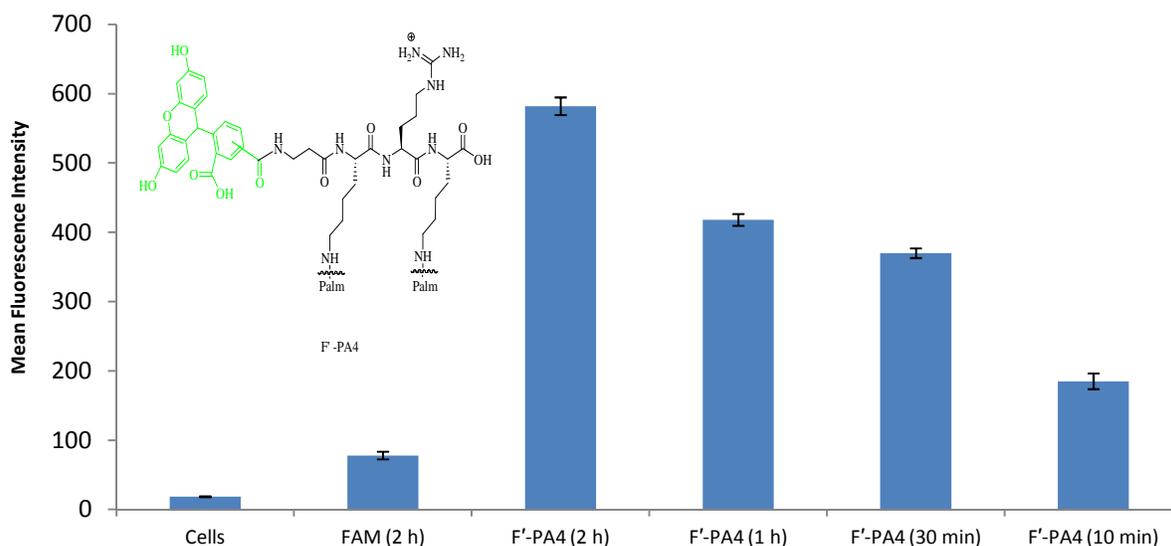

Figure 7. Cellular uptake of F′-PA4 (5 µM) versus FAM (5 µM)

To investigate intracellular location of PA4, F′-PA4 (5 µM) was incubated with SK-OV-3 for 2 h. DAPI was employed to stain the nucleus of cells. Confocal microscopy showed significantly higher fluorescence signal for F′-PA4 versus the corresponding fluorescence marker (FAM) as shown by overlaid picture with DAPI (Figure 8). Most of the fluorescence signal was appeared in the cytoplasm. However, the nucleus of some cells also showed the localization of the F′-PA4. The conjugated fluorescein could increase the hydrophobicity of the PA causing different cellular uptake behavior compared to the non-fluorescently labeled PAs.
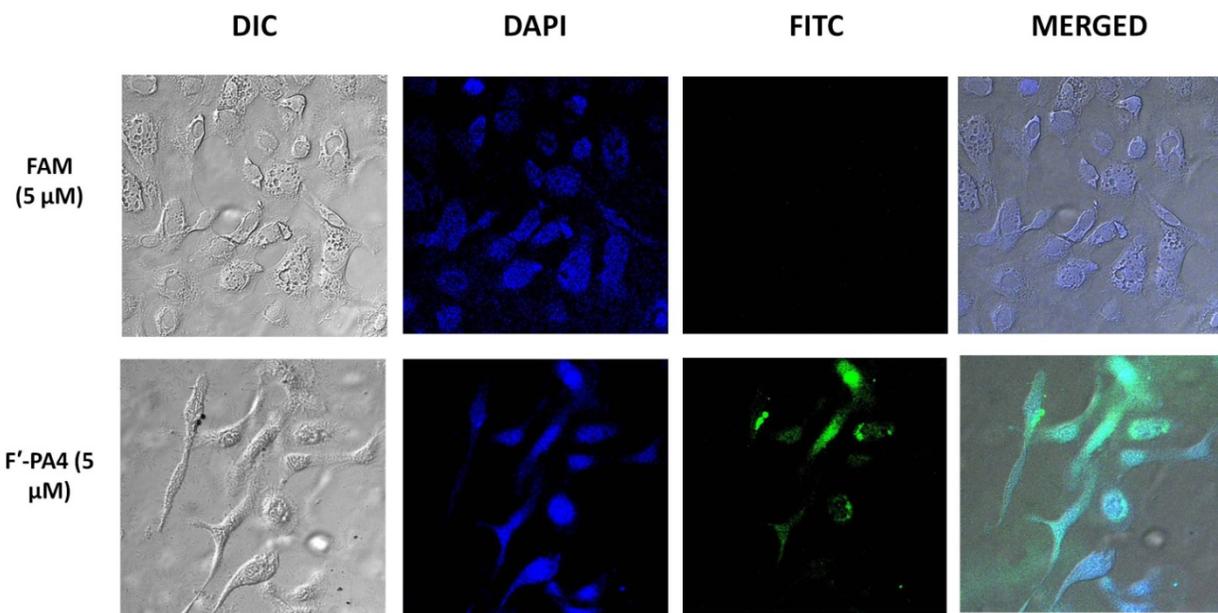
Figure 8. Confocal microscope images of F′-PA4 (5 μM) uptake by SK-OV-3 cells after 2 h incubation.

Understanding the mechanism(s) of the drug cellular uptake has been investigated as one of the important implications for peptide-mediated drug delivery and toxicity. Endocytosis as an energy-dependent process has been introduced as one of the major mechanisms of drug uptake. Different mechanistic pathways could be involved in drug uptake by cells such as phagocytosis, micropinocytosis, and receptor-mediated endocytosis (RME) including clathrin-mediated, caveolae-mediated, and caveolae/clathrin independent endocytosis.[23] Here, the intracellular uptake of fluorescein-labeled peptide, F′-PA4 (5 μM) was evaluated quantitatively in the presence of several inhibitors including, nystatin, chloroquine, chlorpromazine, methyl-β-cyclodextrin, and 5-(*N*-ethyl-*N*-isopropyl)-amiloride (EIA) to investigate the responsible pathway(s) for the uptake.

Chloroquine is a lysosomotropic agent with proportional basic and hydrophobic properties. This compound can cause the pH drop in endosome and block the endosome fusion. Thus, molecular cargos stay in the endosome for a prolonged period. Furthermore, chloropromazine causes the inhibition of clathrin-mediated pathway through translocating clathrin and responsible associated adaptin (PA-2) complex located on the plasma membrane.[24] As it is clear in Figure 9, the intracellular uptake of F′-PA4 was significantly decreased in CCRF-CEM cells in the presence of different endocytic inhibitors including chloroquine and chloropromazine by 3- and 2-fold, respectively, after 2 h incubation, suggesting that the clathrin-mediated pathway is one of the major mechanisms of cellular uptake.

Furthermore, sodium azide is used to block the ATP production by oxidative phosphorylation. In the presence of sodium azide and at 4 ºC, the cellular uptake of F′-PA4 was dropped dramatically, suggesting that the ATP depletion can be the significantly responsible in the internalization process. The presence of the EIA, nystatin, and methyl-β- cyclodextrin did not inhibit the cellular uptake of F′-PA4 proposing that lipid-raft-dependent micropinocytosis, and phagocytosis pathways may not be responsible in the endocytosis process. These results showed that the energy dependent pathways and mainly endocytosis pathways are responsible for transporting the drug across the cell membrane.
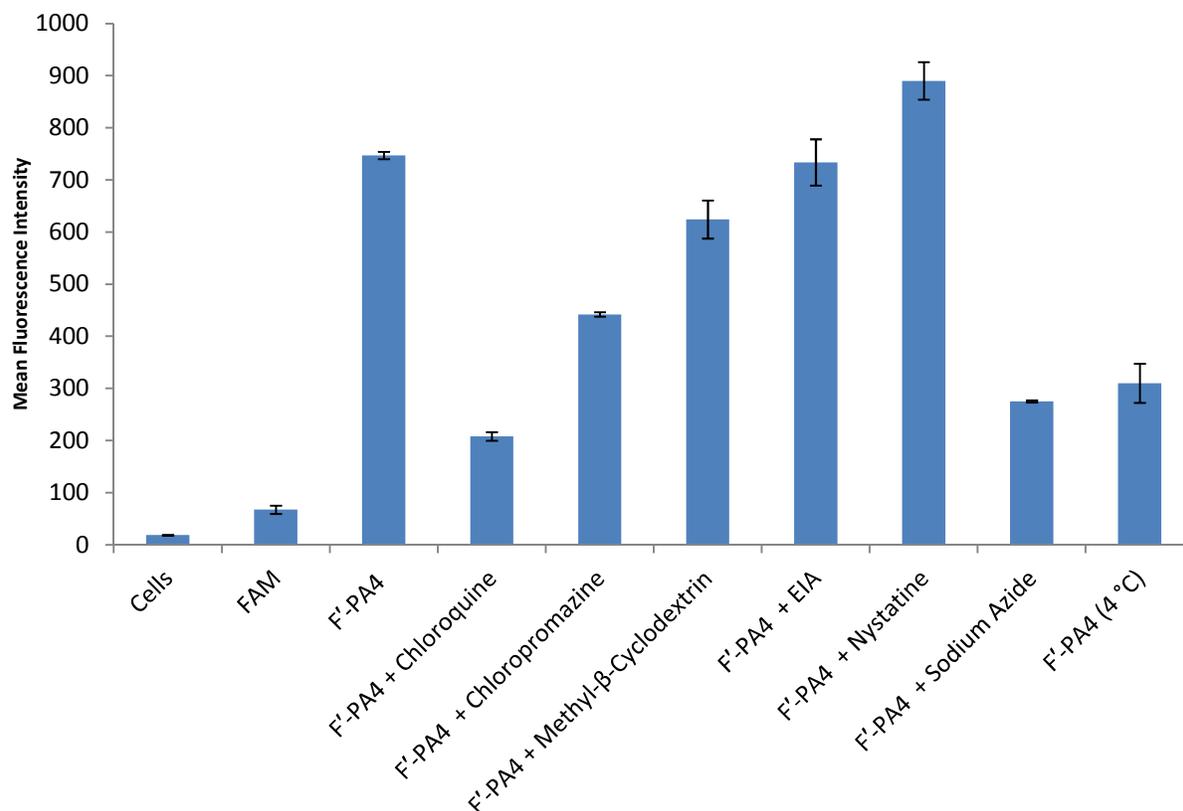
Figure 9. Cellular uptake of F′-PA4 (5 μM) in the absence or presence of different endocytic inhibitors in CCRF-CEM cells after 2 h.

The combination of arginine and palmitic acid in the structure of the PA4 makes the PA an optimal structure compared to other synthesized peptides for crossing over the cellular membrane. The interactions of arginine residues with the corresponding negatively charged phospholipids in lipid bilayer could be critical to trigger the internalization of PA4 into the cell membrane. Hydrophobic interactions generated by palmitic acid carbon chain and the lipids can potentially distort the outer phospholipid monolayer. This process will be followed by PA internalization and enhanced cellular uptake of the cargo molecules. The length of the carbon chain in PA4 is an important parameter that can alter the efficiency of PAs uptake by cells.

Circular dichroism (CD) was employed to obtain a better insight about the interaction between PA4 and PEpYLGLD. The secondary structure of the PA was compared before and after the loading with PEpYLGLD. All spectra were corrected for the baseline and the background by subtraction the blank. CD results showed that PA4 (50 μM) loaded with PEpYLGLD (5 μM) exhibited a different CD pattern compared to those of PA4 (50 μM) and PEpYLGLD (5 μM) alone.
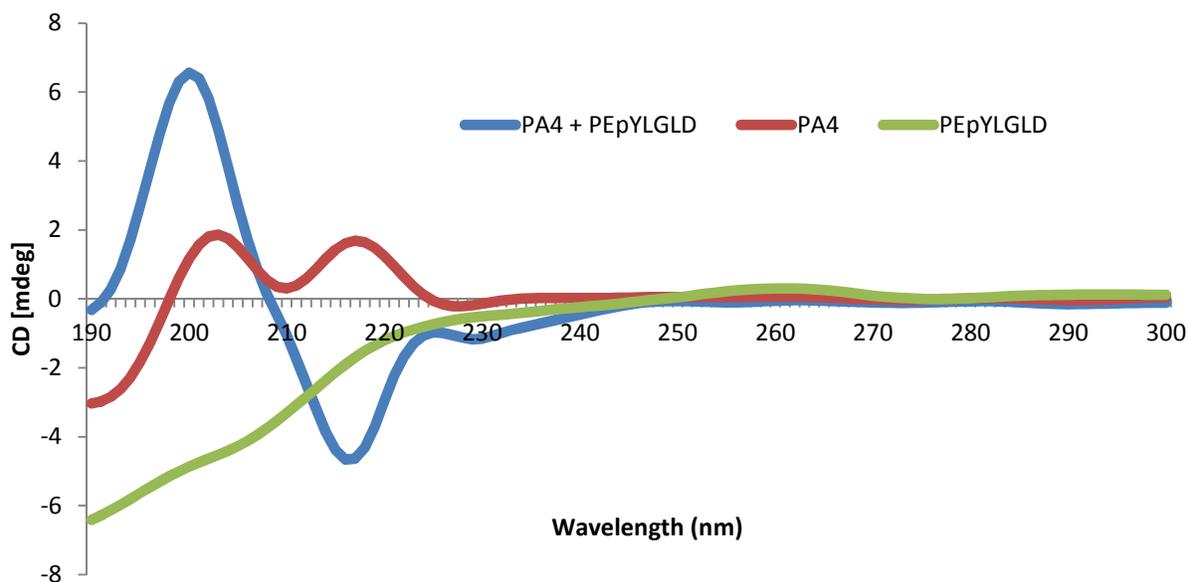

Figure 10. CD pattern of PEpYLGLD and PA4 compared to that of PEpYLGLD-loaded PA4.

PA4 showed two maximum peaks at 203 nm and 218 nm, suggesting that the carrier does not form a classic secondary structure (Figure 10). However, when PA4 was loaded with PEpYLGLD, the CD results showed a similar pattern to β-sheet by a maximum at 199 nm and a minimum at 216 nm, suggesting that the secondary structure formation upon binding with in PEpYLGLD. As it is shown in Figure 10, PEpYLGLD did not show any specific secondary structure. These results confirmed that the interaction between the phosphopeptide and the carrier leads to the formation of a new secondary structure that could be a favorable secondary

structure for cell-penetrating peptides. Furthermore, similar experiment was carried out by using Dox as a drug. The results confirmed that the secondary structure of PA4 is changed upon interactions with the drug (**Figure S2**).

Intracellular Release of Dox

The kinetic pattern of the drug release by PA4 in cells was studied by using Dox as a model drug. The intracellular release of Dox in the presence of PA4 in CCRF-CEM cells was monitored by using HPLC after different incubation times. The CCRF-CEM cells (1×10^7) were incubated with Dox (5 μM)-loaded PA4 (50 μM) for different periods of time including 2, 12, 24, and 48 h. HPLC analysis at 490 nm and at specific time intervals after cellular lysis was used to measure the quantity of the released Dox. The data exhibited that the release of Dox was occurred in a time-dependent manner. HPLC data showed that approximately 3, 6, 11, and 34% of Dox was released intracellularly within 2, 12, 24, and 48 h. These data suggest that Dox-loaded PA4 can be used as a potential prodrug for the sustained release of Dox.

Antiproliferative Assay

To determine whether PA4 can be exploited for the delivery of biologically relevant doses of Dox to cells, the antiproliferative activity of Dox was evaluated in SK-OV-3 cells in the presence and absence of the peptide. The antiproliferative activity of Dox (5 μM) in the presence of the PA4 was improved by approximately 10% compared to that of Dox alone after 24 incubation (Figure 11).
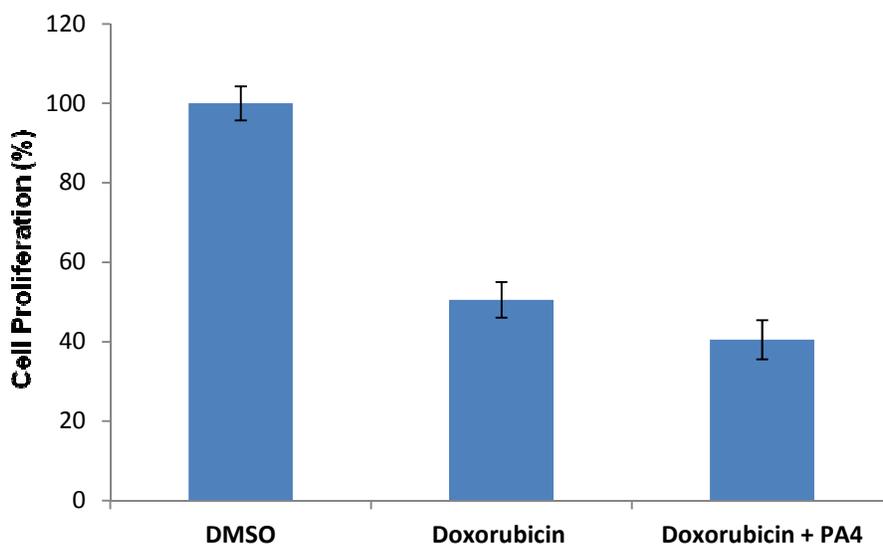
Figure 11. Antiproliferative activity of Dox in the presence of PA4.

An inhibitory effect on the cell proliferation of SK-OV-3 cells suggests improved efficacy of the compound. PA4 alone did not show any toxicity in SK-OV-3 cells under similar conditions, suggesting that the higher antiproliferative is possibly related to the enhanced uptake of the drug in the presence of the PA and intracellular release of Dox.

Conclusion

In conclusion, a new class of PAs containing arginine and lysine conjugated with fatty acyl chains was synthesized. Among all synthesized PAs, only the one with two fatty acyl chains of C_{16} (PA4) showed significantly different biological behavior in the delivery of different cargo

molecules. Furthermore, PA4 showed minimal toxicity at 100 μM. PA4 was able to act as a molecular transporter of fluorescence-labeled 3TC and a phosphopeptide (PEpYLGLD) intracellularly. High cellular internalization of the labeled drugs by PA4 suggests the potential application of PA4 as a molecular transporter. Confocal microscopy showed that PA4 deliver the majority of cargos to the cytoplasm in cells. The present results provide insights for further optimization of PAs in this class as cellular delivery transporter.

Supporting Information

Additional supporting figures for cytotoxicity of peptide amphiphiles, CD pattern of PA4 compared to that of Dox-loaded PA4, and HPLC profile for intracellular release of Dox. This material is available free of charge via the Internet at http://pubs.acs.org.

ACKNOWLEDGMENTS

REFERENCES

1. a) Peterfreund, R. A.; Philip, J. H. Critical parameters in drug delivery by intravenous infusion. *Expert Opinion on Drug Delivery* **2013**, In Press, DOI: 10.1517/17425247.2013.785519. b) Vonarbourg, A.; Passirani, C.; Saulnier, P.; Benoit, J.-P.

Parameters influencing the stealthiness of colloidal drug delivery systems, *Biomaterials* **2006**, 27, 4356–4373

2. a) Kim, J.-K.; Anderson, J.; Jun, H.-W., Repka, M. A.; Jo, S. Self-assembling peptide amphiphile-based nanofiber gel for bioresponsive cisplatin delivery, *Molecular Pharmaceutics* **2009**, 6, 978-985. b) Tan, A.; Rajadas, J.; Seifalian, A. M. Biochemical engineering nerve conduits using peptide amphiphiles, *Journal of Controlled Release* 163, **2012**, 342–352. c) Javali, N. M.; Raj, A.; Saraf, P.; Li, X.; Jasti, B. Fatty acid–RGD peptide amphiphile Micelles as potential paclitaxel delivery carriers to αvβ3Integrin overexpressing tumors, *Pharm. Res*. **2012**, 29, 3347–3361. d) Wiradharma, N.; Tong, Y. W.; Yang, Y.-Y. Design and evaluation of peptide amphiphiles with different hydrophobic blocks for simultaneous delivery of drugs and genes, *Macromol. Rapid Commun*. **2010**, 31, 1212–1217. e) Matson, J. B.; Newcomb, C. J.; Bitton, R.; Stupp, S. I. Nanostructure-templated control of drug release from peptide amphiphile nanofiber gels, *Soft Matter* **2012**, 8, 3586–3595.

3. Bulut, S.; Erkal, T. S.; Toksoz, S.; Tekinay, A. B.; Tekinay, T.; Guler, M. O. Slow release and delivery of antisense oligonucleotide drug by self-assembled peptide amphiphile nanofibers. *Biomacromolecules* **2011**, 12, 3007–3014.

4. Hess, G. T.; Humphries, W. H. T.; Fay, N. C.; Payne, C. K. Cellular binding, motion, and internalization of synthetic gene delivery polymers, *Biochim. Biophys. Acta*. **2007**, 1773, 1583–1588.

5. Wiethoff, C. M.; Koe, J. G.; Koe, G. S.; Middaugh, C. R. Compositional effects of cationic lipid/DNA delivery systems on transgene expression in cell culture, *J. Pharm. Sci.* **2004**, 93, 108–123.

6. L. Haines-Butterick, K. Rajagopal, M. Branco, D. Salick, R. Rughani, M. Pilarz, M. S. Lamm, D. J. Pochan, J. P. Schneider, Controlling hydrogelation kinetics by peptide design for three-dimensional encapsulation and injectable delivery of cells. *Proc. Natl. Acad. Sci. U. S. A.* **2007**, 104, 7791–7796.

7. Thornton, P. D.; Mart, R. J.; Webb, S. J.; Ulijn, R. V. Enzyme-responsive hydrogel particles for the controlled release of proteins: designing peptide actuators to match payload, *Soft Matter*, **2008**, 4, 821–827.

8. Bulut, S.; Erkal, T. S.; Toksoz, S.; Tekinay, A. B.; Tekinay, T.; Guler, M. O. Slow release and delivery of antisense oligonucleotide drug by self-assembled peptide amphiphile nanofibers, *Biomacromolecules*, **2011**, 12, 3007–3014.

9. Nasrolahi Shirazi, A.; Tiwari, R. K.; Oh, D.; Banerjee, A.; Yadav, A.; Parang, K. Efficient Delivery of cell impermeable phosphopeptides by a cyclic peptide amphiphile containing tryptophan and arginine. *Mol Pharm.* **2013,** 10, 2008–2020.

10. Soukasene, S.; Toft, D. J.; Moyer, T. J.; Lu, H. M.; Lee, H. K.; Standley, S. M.; Cryns, V. L.; Stupp, S. I. Antitumor activity of peptide amphiphile nanofiber-encapsulated camptothecin. *ACS Nano*, **2011**, 5, 9113–9121.

11. Guler, M.; Claussen, R.; Stupp, S.I. Encapsulation of pyrene within self-assembled peptide amphiphile nanofibers, *J. Mater. Chem.* **2005**, 15, 4507–4512.

12. Accardo, A.; Tesauro, D.; Mangiapia, G.; Pedone, C.; Morelli, G. Nanostructures by self-assembling peptide amphiphile as potential selective drug carriers, *Biopolymers* **2007**, 88, 115–121.

13. Kim, J. K.; Anderson, J.; Jun, H. W.; Repka, M. A.; Jo, S. Self-assembling peptide amphiphile-based nanofiber gel for bioresponsive cisplatin delivery. Mol. Pharm. 2009, 6, 978–985.

14. a) Gupta, A.; Mandal, D.; Ahmadibeni, Y.; Parang, K.; Bothun, G. Hydrophobicity drives the cellular uptake of short cationic peptide ligands. *Eur. Biophys. J*. **2011**, 40, 727–736. b) Ye, G.; Gupta, A.; DeLuca, R.; Parang, K.; Bothun, G.D. Bilayer disruption and liposome restructuring by a homologous series of small Arg-rich synthetic peptides, *Coll. Surf. B: Biointerfaces* **2010**, 76, 76–81.

15. Lundberg, P.; El-Andaloussi, S.; Sutlu, T.; Johansson, H.; Langel, U. Delivery of short interfering RNA using endosomolytic cell- penetrating peptides. *FASEB*. **2007**, 21, 664–671.

16. Mandal, D.; Nasrolahi Shirazi, A.; Parang, K. Cell-penetrating homochiral cyclic peptides as nuclear-targeting molecular transporters**.** *Angew. Chem. Int. Ed*., **2011**, 50, 9633−9637.

17. (a) Nasrolahi Shirazi, A.; Tiwari, R. K.; Brown, A.; Mandal, D.; Sun, G.; Parang, K. Cyclic peptides containing tryptophan and arginine as Src kinase inhibitors. *Bioorg. Med. Chem. Lett.* **2013**, 23, 3230−3234. (b) Nasrolahi Shirazi, A.; Tiwari, R. K.; Chhikara, B. S.; Mandal, D. Parang, K. Design and biological evaluation of cell-penetrating peptide–doxorubicin conjugates as prodrugs. *Mol. Pharm.* 2013, **10**, 500–511.

18. Cai, H.; Yao, P. In-situ preparation of gold nanoparticle-loaded lysozyme-dextran nanogels and applications for cell imaging and drug delivery. *Nano Scale* **2013**, 5, 2892–2900.

19. (a) Massard, J.; Benhamou, Y. Treatment of chronic hepatitis B in HIV co-infected patients. *Gastroenterol. Clin. Biol.* **2008**, 32, S20–S24. (b) Saag, M. S. Emtricitabine, a new antiretroviral

agent with activity against HIV and hepatitis B virus. *Clin. Infect. Dis.* **2006**, 42, 126–131. (c) Nelson, M.; Schiavone, M. Emtricitabine (FTC) for the treatment of HIV infection. *Int. J. Clin. Pract.* **2004**, 58, 504–510.

20. Agarwal, H. K.; Chhikara, B. S.; Hanley, M. J.; Ye, G.; Doncel, G. F.; Parang, K. Synthesis and biological evaluation of fatty acyl ester derivatives of (-)-2',3'-dideoxy-3'-thiacytidine. *J. Med. Chem.* **2012**, 55, 4861–4871.

21. Agarwal, H. K.: Chhikara, B. S.: Bhavaraju, S.: Mandal, D.: Doncel, G. F.: Parang, K. Emtricitabine prodrugs with improved anti-HIV activity and cellular uptake. *Mol. Pharm.* **2013**, 10, 467–476.

22. Machida, K.; Mayer, B. J. The SH2 domain: versatile signaling module and pharmaceutical target. *Biochim. Biophys. Acta* **2005**, 1747, 1–25.

23. Conner, S. D.; Schmid. S. L. Regulated portals of entry into the cell, *Nature* **2003**, 422, 37–44.

24. (a) Madani, F.; Lindberg, S.; Langel, U.; Futaki, S.; Gra☐slund, A. Mechanisms of cellular uptake of cell-penetrating peptides. *J. Biophys*. **2011**, 2011, 414729. (b) Nasrolahi Shirazi, A.; Tiwari, R. K.; Oh, D.; Sullivan, B.; McCaffrey, K.; Mandal, D.; Parang, K. Surface decorated gold nanoparticles by linear and cyclic peptides as molecular transporters. *Mol. Pharm*. **2013**, 10, 3137–3151.